# Laser fluorescence study of AlO formed in the reaction Al + $O_2$: Product state distribution, dissociation energy, and radiative lifetime

P. J. Dagdigian*, H. W. Cruse†, and R. N. Zare

*Department of Chemistry, Columbia University, New York, New York 10027*
(Received 21 October 1974)

The reaction Al + $O_2$ → AlO + O has been investigated by the method of laser-induced fluorescence. Excitation spectra are reported for AlO products formed under single-collision conditions in a "beam-gas" arrangement. The relative vibrational populations (proportional to total cross sections for formation), as well as the relative rotational populations for the $v = 0$ and $v = 1$ vibrational levels, are derived. The rotational distributions are found to differ significantly, with $v = 0$ having more rotational excitation than $v = 1$. The vibrational distribution is non-Boltzmann, the falloff with $v > 1$ exceeding $v = 1$ compared to $v = 0$. The observed internal state distributions are compared with those calculated from phase space theory. It is concluded tentatively that the partitioning of the Al + $O_2$ reaction energy among the product modes is not governed solely by statistical considerations. The dynamics of the Al + $O_2$ reaction are compared with those of the exothermic Ba + $O_2$ and endothermic K + $O_2$ reactions. From a knowledge of the AlO internal states populated by the Al + $O_2$ reaction and from an estimate of the thermal reactant energies, a lower bound for the ground state dissociation energy of AlO is derived. By combining the present lower bound with the upper bound previously derived from observation of the onset of an AlO absorption continuum, the value $D_0^0(\mathrm{AlO}) = 121.5 \pm 1$ kcal/mole is recommended for aluminum monoxide. Direct measurement of the fluorescence decay of the AlO B $^2\Sigma^+$ state as a function of time after excitation by the short (~5 nsec) laser pulse has allowed the determination of the radiative lifetimes $\tau(v' = 0) = 100 \pm 7$ nsec, $\tau(v' = 1) = 102 \pm 7$ nsec, and $\tau(v' = 2) = 102 \pm 4$ nsec, where the error estimates represent three standard deviations.

## I. INTRODUCTION

Although the combustion of metals has long been a fruitful topic in chemical research, the gas-phase oxidation process $M + O_2 \rightarrow MO + O$ is usually an endothermic reaction. Consequently, most combustion studies of metals involve heterogeneous reactions that are difficult to characterize. An important exception is the oxidation of aluminum atoms by $O_2$. Recently the kinetics of the homogeneous gas-phase reaction $Al + O_2 \rightarrow AlO + O$ has been studied by Fontijn, Felder, and Houghton[1] in a fast-flow reactor. They find that this reaction proceeds with a rate coefficient $k$ of $3 \pm 2 \times 10^{-11}$ cm$^3$ molecule$^{-1}$ sec$^{-1}$ which shows no measurable temperature variation over the range 1000–1700 °K. Thus to within their experimental error, $Al + O_2$ has no activation energy. In addition, from the magnitude of $k$ it appears that chemical reaction occurs for one collision in ten.

We report here the internal state distribution of the ground state AlO products formed when a beam of Al atoms traverses a scattering chamber filled with $O_2$ gas at a pressure of less than $2 \times 10^{-4}$ torr ("beam-gas" arrangement).[2] Under these conditions, the initial internal state distribution of the AlO product is collisionally unrelaxed and may be determined from laser-induced fluorescence excitation spectra.[3] The AlO $B^2\Sigma^+ - X^2\Sigma^+$ bands, which lie in the blue green, are very convenient for this purpose. Knowledge of the internal state distribution, namely, the relative population (total cross section for formation) of the rotation–vibration levels of the AlO $X$ state which are energetically accessible, provides information on the dynamics of this simple bimolecular reaction. Unfortunately, comparison of the experimental and theoretical internal state distributions is rendered somewhat difficult because the large thermal spread in the initial translational energy $E^i_{\mathrm{trans}}$ is comparable to the exothermicity of this nearly thermoneutral reaction. An expression for the distribution of $E^i_{\mathrm{trans}}$ is derived for the present experimental arrangement and is used to average the theoretical distributions.

In addition, energy balance for the $Al + O_2$ reaction may be used to derive a lower bound to the dissociation energy $D_0^0(\mathrm{AlO})$ of the aluminum monoxide ground state. This lower bound, when combined with the upper bound previously obtained from observation of the onset of an AlO absorption continuum, allows one to make a new extimate of $D_0^0(\mathrm{AlO})$. Finally, the radiative lifetime of the AlO $B^2\Sigma^+$ state may be measured in a direct manner since the AlO fluorescence is excited by a tunable pulsed dye laser with a pulse width that is small compared to the characteristic time for fluorescence decay.

## II. EXPERIMENTAL

The apparatus employed in the present experiments is very similar to that used for the previous study[4] of the reactions $Ba + O_2 \rightarrow BaO + O$ and $Ba + CO_2 \rightarrow BaO + CO$. The high-temperature oven is modified so that a beam of aluminum can be produced. A tantalum tube (2.5 cm diam., 17 cm long, 0.025 cm wall thickness) is used as the heater and is surrounded by four tantalum foil heat shields. The crucible containing the aluminum is mounted inside the heater and is maintained at a temperature of about 1600 °K (corrected pyrometer reading) corresponding to a pressure of about 0.16 torr.[5] Molten aluminum at this temperature is extremely corrosive. However, boron nitride (Union Carbide) proves to be a very satisfactory container material. Aluminum vapor

 

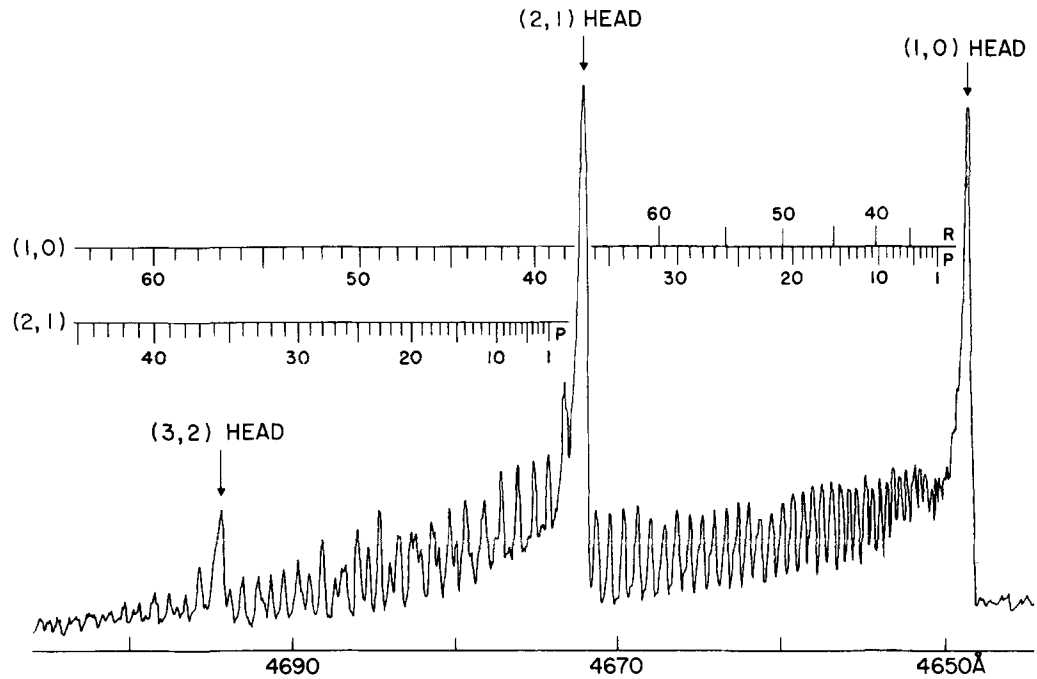


FIG. 1. AlO excitation spectrum of the $B^2\Sigma^+ - X^2\Sigma^+$ $\Delta v = +1$ sequence for the Al + $O_2$ reaction. The heads of the $(v', v)$ bands are noted. The unresolved $P_1$ and $P_2$ doublets of the (1, 0) and (2, 1) bands are denoted as $P(N)$. In addition, the location of the (1, 0) $R_1$ and $R_2$ doublets, denoted $R(N)$, are indicated. The spectrum was taken with the dye 7-diethylamino-4-methylcoumarin.

is also very reactive and the tantalum heater tube must be replaced after several runs. The aluminum beam enters the scattering chamber filled with $O_2$ at pressures of $\leq 8\times 10^{-4}$ torr ("beam-gas" arrangement), and the AlO product is detected by laser-induced fluorescence. By comparison of experimental excitation spectra, it is found that collisional relaxation of the initial AlO internal state distribution is negligible at $O_2$ pressures $\leq 3\times 10^{-4}$ torr. Accordingly, excitation spectra are taken with $O_2$ pressures of $2\times 10^{-4}$ torr or less (uncorrected ionization gauge readings).

A Molectron dye laser system (UV-300 nitrogen laser, DL-200 dye module, and home-built wavelength drive)[4] is employed as the fluorescence excitation source. Dyes used are 7-diethylamino-4-methylcoumarin (bandwidth 0.15 Å) for the AlO $\Delta v = v' - v = +1$ sequence and CSA-22[6] (bandwidth 0.4 Å) for the $\Delta v = -1$ sequence. (Excited state quantum numbers are written with one prime, while ground state quantum numbers are denoted with no primes.) The laser beam intersects the Al beam; no angular distribution measurements have been made. At full laser power the effects of optical pumping on the excitation spectra[7] are clearly discernible: (1) The fluorescence intensity at a given wavelength is not linearly proportional to laser power and (2) the relative intensities of rotational lines from different $(v', v)$ bands change with increasing laser power. In order to minimize optical pumping, the laser power is reduced using neutral density filters (Oriel) until no change in the relative intensities of different lines in the excitation spectrum could be discerned with further reduction in laser power.

Gated detection electronics are employed. Two different boxcar integrators are used for different aspects of this study. A PAR model 162 with model 164 plug-in is employed with gate width of 500 nsec (several times the AlO radiative lifetime) to obtain the excitation spectrum in the kinetic studies. The boxcar integrator and nitrogen laser are both triggered from a pulse generator, and the boxcar gate is opened ~30 nsec before the laser pulse. A PAR model 160 is used with a 10 nsec gate width for measurements of the AlO $B$ state lifetime. The boxcar time base is calibrated to better than 1% using a signal generator and digital counter. In both the kinetic and lifetime studies, repetitive scans are taken and the results averaged in order to compensate for the slow drift in time of the Al beam intensity. The beam intensity is monitored between scans by measuring the total AlO fluorescence with a wide (500 nsec) gate. A photodiode is used in the kinetic studies to measure the variation of laser intensity with laser wavelength, and the fluorescence signal is normalized to a constant laser intensity. In order to reduce the contribution of light from the Al oven to the signal, a blue Corning filter (4-97) is placed directly in front of the photomultiplier. This also eliminates the unwanted possibility of observing AlO $B-A$ or $A-X$ fluorescence but does not affect the AlO $B-X$ fluorescence.

## III. DETERMINATION OF AlO INTERNAL STATE DISTRIBUTION

The AlO $B^2\Sigma^+ - X^2\Sigma^+$ band system is used for product state analysis of AlO produced by the Al + $O_2$ reaction. Figures 1 and 2 present typical excitation spectra for the $\Delta v = +1$ and $-1$ sequences, respectively. Figure 3 shows a continuation of the $\Delta v = -1$ sequence, taken at five times higher laser power than for Fig. 2 in order to observe weaker features. The bandheads, formed by the $R_1$ and $R_2$ branches[8] (the bandhead occurs from $N = 14$

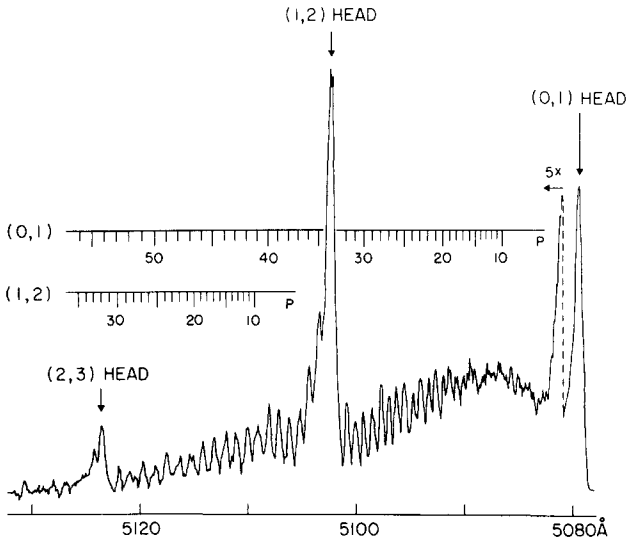


FIG. 2. AlO excitation spectrum of the $\Delta v = -1$ sequence for the $Al + O_2$ reaction. The spectral region to the red of the (0, 1) bandhead was recorded at a factor of 5 greater sensitivity, and the dye CSA-22 was used.

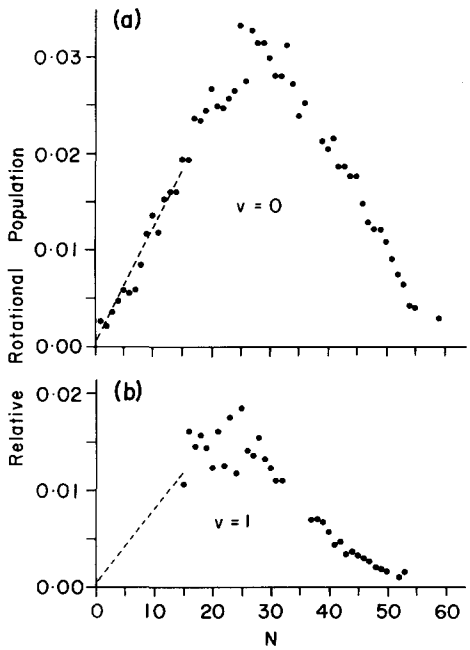


FIG. 4. Derived relative rotational populations for AlO molecules from the $Al + O_2$ reaction produced in the (a) $v = 0$ and (b) $v = 1$ vibrational levels. The total population in each vibrational level has been normalized to the relative vibrational populations so that the population of any $(v, N)$ level is directly comparable to that of any other level. The dashed lines denote the $2N+1$ proportionality expected for the population of low $N$ levels.

to 22 for the various $(v', v)$ bands used), are prominent in the spectra. The experimentally resolved $P$ branch members offer an opportunity to determine individual rotational populations. The $P$ lines are actually unresolved doublets $P_1$ and $P_2$. However, we assume that the chemical reaction populates the spin components $J = N - \frac{1}{2}$ and $J = N + \frac{1}{2}$ in the ratio of their degeneracies. We have concentrated our attention on the $\Delta v = +1$ and $-1$ sequences because the Franck–Condon factors[9] are large and, more importantly, they do not change drastically with $v$. This last fact helps us to minimize the effect of optical pumping.

It is of great interest to determine whether the rotational distribution varies as a function of $v$ level. We have used the resolved $P$ lines of the (1, 0) and (0, 1) bands to deduce the rotational distributions for molecules produced in the $v = 0$ and 1 levels. Distributions in higher $v$ levels have not been obtained because of the weakness of the bands and because of the interference from $v = 0$ and 1 bands (see Figs. 1–3).

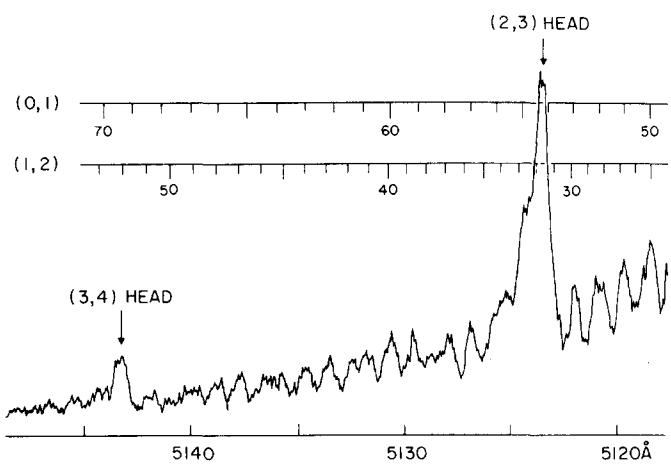


FIG. 3. AlO excitation spectrum of the $\Delta v = -1$ sequence for the $Al + O_2$ reaction. This continuation of Fig. 2 was taken at five times higher laser power.

The peak intensities of the $P$ lines above the "background" are not directly proportional to the populations of their respective $N$ levels for three reasons. First, the $P$ lines at low $N$ do not stand out above the $R$ branch "background." In fact, we see that the $P$ lines of the $\Delta v = -1$ sequence close to the band origin (see Fig. 2) cannot be resolved for $N \leq 10$ as a result of the relatively large laser bandwidth. Second, the peak heights at high $N$ appear reduced in amplitude because of the splitting of the spin components which increases linearly with $N$. For example, at $N = 50$ the spin splitting amounts to about 0.69 $cm^{-1}$ in the (1, 0) band, causing the width of the line to be broadened and the peak height to be depressed. Finally, at low to intermediate $N$, $R$ lines of high $N$ go in and out of coincidence with the $P$ lines.

However, we may determine correction factors by which the $P$ line intensities must be multiplied in order to be proportional to populations.[10] This is accomplished in an iterative manner using computer-generated spectra. First a set of rotational populations (obtained from the peak heights) are assumed. Then the AlO line positions[11] are convoluted with a Gaussian bandwidth function having the experimental FWHM. The correction factors are then obtained by comparing the calculated $P$ line intensities with the assumed rotational populations. Since these factors are somewhat dependent on the assumed populations, the latter are varied so that the calculated spectrum resembles closely the experimental spectrum.

TABLE I. Relative[a] AlO vibrational populations $N_v$ for the $Al + O_2$ reaction.

| $v$ | $N_v$ |
|---|---|
| 0 | (1.00) |
| 1 | 0.44 ± 0.02 |
| 2 | 0.086 ± 0.005 |
| 3 | 0.013 ± 0.002 |
| 4 | 0.003 ± 0.001 |

[a]Populations have been normalized so that $N_0$ is unity.

Figure 4 presents the derived rotational populations for the $v = 0$ and 1 levels. For $v = 0$, the populations of low $N$ levels appear to be proportional to $2N + 1$ [dashed line in Fig. 4(a)]. As discussed[4,12] in connection with BaO, this is the expected behavior for low $N$. We cannot determine the low $N$ populations for $v = 1$ because of the larger laser bandwidth used for the (0, 1) band. Nevertheless, we have drawn in a dashed line to indicate the likely low $N$ populations, assuming the $2N + 1$ proportionality found for $v = 0$. We can see clearly from Fig. 4 that the rotational distributions of the two vibrational levels are significantly different and that the $v = 0$ level has more rotational excitation.

Once rotational populations have been obtained, it is straightforward to deduce vibrational populations from relative band head intensities. For simplicity, we assume the rotational distributions in the $v > 1$ levels are the same as in the $v = 1$ level. The deduced relative vibrational populations are tabulated in Table I. The populations cannot be fit to a vibrational temperature since the falloff at high $v$ is much greater than that for $v = 1$ relative to $v = 0$.

## IV. RADIATIVE LIFETIME: $\tau(\mathrm{AlO}\, B\,^2\Sigma^+)$

The dye laser has a pulse width of about 5 nsec. Hence it is possible to measure directly radiative lifetimes by observing the decay of the fluorescence signal with time. Since the molecules are present in low concentration under collision-free conditions, this technique is free from most systematic errors, such as radiative trapping, quenching, and cascading, which have plagued measurements of radiative lifetimes in the past. Recently we have determined radiative lifetimes to an accuracy of 10% for about 40 electronic states of the alkaline earth monohalides.[13] These measurements were carried out by photographing oscilloscope traces of the fluorescence decay resulting from single laser shots. The present study of the AlO $B\,^2\Sigma^+$ lifetime is similar to our previous work but differs in that we use a boxcar integrator. As in the kinetics studies, the boxcar and dye laser are both triggered from a pulse generator. The boxcar gate is only 10 nsec wide and is swept in time through the fluorescence decay curve in a period typically of 15 min. Each portion of the plotted curve is then the average of the signal from many laser shots.

Figure 5 shows a typical scan of the fluorescence decay as a function of time. An exponential decay is at once apparent. Individual scans are analyzed to yield lifetimes $\tau_i$ and standard deviations $\sigma_i$ by fitting the logarithm of the signal vs time to a straight line. The effects of the finite photomultiplier risetime and boxcar gate width are minimized by ignoring the first 75 nsec of each scan. The individual $\tau_i$ (6 to 10 in number) are averaged in a weighted manner to obtain lifetimes $\tau$ for each $v'$ level:

$$\tau = \sum_i \tau_i \sigma_i^{-2} / \sum_i \sigma_i^{-2}.$$

Table II presents the values of $\tau$ obtained for the $v' = 0$ to 2 levels of the AlO $B$ state. In all cases, the laser wavelength is set to coincide with a bandhead, indicated in Table II. We believe we have measured the radiative lifetime of the AlO $B$ state to an accuracy of a few percent. The variation of the lifetime with $v'$ level is seen to be small compared with the experimental uncertainties.

The determination of absolute molecular radiative properties such as oscillator strengths and lifetimes is fraught with much difficulty and controversy. This is especially true for high-temperature reactive species such as AlO. Table III summarizes all known determinations of the AlO $B$–$X$ (0, 0) oscillator strength. The experimental methods may be divided into two categories: (1) absolute intensity measurements, which require a knowledge of the AlO concentration, and (2) time-resolved fluorescence decay, which requires that all molecules excited to the state of interest be formed initially in that state and removed only by radiative decay. Vanpee, Kineyko, and Caruso[14] and Hooker and

TABLE II. Radiative lifetimes as a function of vibrational level $v'$ for the AlO $B\,^2\Sigma^+$ state.

| | Excitation band | | |
|---|---|---|---|
| $v'$ | $(v', v'')$ | λ(Å) | $\tau$(nsec)[a] |
| 0 | 0, 0 | 4842 | 100 ± 7 |
| 1 | 1, 0 | 4648 | 102 ± 7 |
| 2 | 2, 1 | 4672 | 102 ± 4 |

[a]The error limits are $\pm 3\sigma$ of the fits.

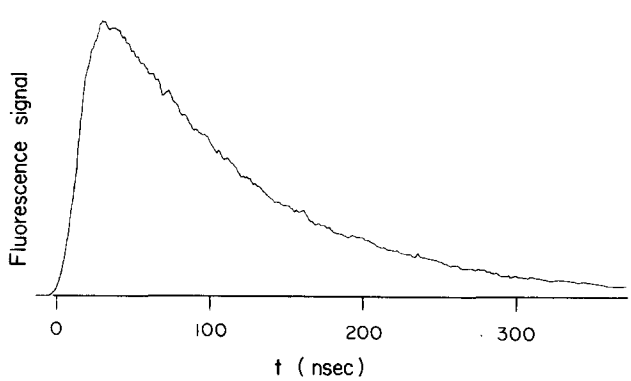


FIG. 5. Scan of AlO $B\,^2\Sigma^+$ $v' = 0$ fluorescence decay with time. The (0, 0) band at 4648 Å has been employed for excitation. This trace was obtained using a boxcar integrator with a 10 nsec gate width. The lifetime determined from this particular trace is 102 ± 5 nsec.

TABLE III. Experimental and theoretical determinations of the AlO $B-X$ (0, 0) oscillator strength. No error estimates are given here.

| Investigators | Method | $f_{00}$ |
|---|---|---|
| Vanpee, Kineyko, and Caruso[a] | flame emission absolute-intensity measurement | 0.0027 |
| Wentink, Pederson, and Diebold[b] | laser blowoff fluorescence decay | 0.0098 |
| Hooker and Main[c] | shock tube absorption measurement | 0.0035 |
| Johnson, Capelle, and Broida[d] | laser-induced fluorescence decay | 0.021 |
| Michels[e] | *ab initio* configuration interaction calculation | 0.012 |
| Yoshimine, McLean, and Liu[f] | *ab initio* configuration interaction calculation | 0.074 |
| Dagdigian, Cruse, and Zare[g] | laser-induced fluorescence decay | 0.027 |

[a]Reference 14. [b]Reference 16. [c]Reference 15. [d]Reference 17. [e]Reference 18. [f]Reference 19. [g]This work.

Main[15] have made absolute intensity measurements to determine $f_{00}$. These measurements are extremely difficult and are subject to large systematic errors caused by uncertainties in the determination of the AlO concentration.

The fluorescence decay measurements of Wentink, Pederson, and Diebold,[16] Johnson, Capelle, and Broida,[17] and the present work are inherently simpler in that no knowledge of the absolute AlO concentration is required. Instead, however, it must be ensured that the operating pressures are so low that radiation trapping and electronic quenching are negligible. In addition, all AlO $B$ state molecules must be produced in a time very short compared to the radiative lifetime so that the effects of cascade or collisional excitation are insignificant. Of the three fluorescence decay determinations, the radiative lifetime (272 ± 14 nsec) found from the laser blowoff study stands out by a factor of ~2.5 from the other laser-induced fluorescence measurements. Evidently the criteria for the application of the direct fluorescence decay method is not well met for laser blowoff. Since we are not able to model the processes occurring in laser blowoff, we are unable to assess the source of the difficulty. The lifetime results for the $v' = 0$ level of Johnson *et al.* (128.6 ± 6.0 nsec) and of the present study (100 ± 7 nsec) are within 30% of one another, but they do not agree within their combined error estimates. Both studies involve excitation of AlO by a nitrogen laser pumped tunable pulsed dye laser, and in both cases the AlO is produced by the reaction $Al + O_2$. However, the work of Johnson *et al.* differs from ours in that (1) they observe the fluorescence decay from single laser shots on an oscilloscope and (2) their operating pressures are much higher. They find no change in the observed AlO radiative lifetime on varying the AlO density by a factor of 2 and on varying the gas pressure from 0.25 to 50 torr for He, 0.8 to 20 torr for $N_2$, and 0.01 to 10 torr for $O_2$. They conclude that radiation trapping and electronic quenching of AlO are negligible under their conditions. No acceptable reason for the disparity between the results of Johnson *et al.* and the values found in the present work can be offered at this time, but in defense of the present work it must be pointed out that (1) our measurements are made at much lower pressures ($2 \times 10^{-4}$ torr) where effects caused by collisions or by radiation entrapment are expected to be negligible and (2) extensive checks for systematic errors of the sort described in the alkaline earth monohalide studies[13] were carried out.

There have been two *ab initio* calculations of the AlO $B-X$ oscillator strength. Michels[18] obtained the electronic transition moment as a function of internuclear distance from a configuration interaction (CI) calculation (190 configurations of $^2\Sigma^+$ symmetry). Using RKR potentials for vibrational averaging, he found a lifetime of 234 nsec. Most recently, Yoshimine, McLean, and Liu[15] carried out elaborate CI calculations of the $X$, $A$, and $B$ states of AlO. In a more limited (140 configurations) and less accurate CI calculation, they obtained a $B-X$ oscillator strength corresponding to a lifetime of 38 nsec. They state that an error of a factor of ~3 is consistent with the level of approximation employed. Calculation of the AlO $B-X$ oscillator strength severely taxes present computational capabilities because (1) the excited state is of the same symmetry as the ground state and (2) there is no adequate single configuration SCF description of the ground state.[19] It is of great interest to know whether the use of the more elaborate CI wavefunctions of Yoshimine *et al.* would overcome these two problems.

## V. DISSOCIATION ENERGY: $D_0^0$(AlO)

The determination of bond energies for high-temperature transient species has occupied the attention of investigators for many years. All known determinations of $D_0^0$(AlO) are summarized in Table IV, from which it can be seen that there exists a wide spread of values based on various methods. In general, flame photometry results yield high values, spectroscopic extrapolations yield low values, while mass spectrometric determinations are intermediate. In recent years the spread of values has decreased.

Based on the observation of an absorption continuum by Tyte,[20] Drowart[21] has placed an upper bound on the AlO dissociation energy of $D_0^0(\text{AlO}) \leq 122.1 \pm 0.6$ kcal/mole. In addition, it is possible to set lower bounds to bond energies from a study of chemical reactions under single-collision conditions, in which the products are state analyzed. In particular, Gole and Zare[22] have placed the lower bound $D_0^0(\text{AlO}) \geq 118.3 \pm 1.4$ kcal/mole from the AlO chemiluminescence spectrum resulting from the $Al + O_3$ reaction. In an analogous way, we may also set a lower bound from a study of the reaction $Al + O_2$ by laser-induced fluorescence. Indeed, we shall argue that our lower bound, combined with Drowart's upper bound, leads to an equality for $D_0^0$(AlO) with an uncertainty of only ± 1 kcal/mole.

The dissociation energy $D_0^0$(AlO) is defined as the energy required to separate the AlO molecule in the lowest $(v, J)$ level of the ground electronic state into con-

stituent atoms in their lowest internal states. By choosing $Al(^2P) + O(^3P) + O_2(X\,^3\Sigma_g^- v = 0, J = 0)$ as the reference state, we obtain the equality

$$-D_0^0(O_2) + E_{int}(O_2) + E_{trans}^i = -D_0^0(AlO) + E_{int}(AlO) + E_{trans}^f \quad (1)$$

from the application of energy balance to the reaction $Al + O_2 \rightarrow AlO + O$. In Eq. (1) $E_{int}(O_2)$ and $E_{int}(AlO)$ are the internal energies of $O_2$ and AlO, measured from their lowest energy levels, and $E_{trans}^i$ and $E_{trans}^f$ are the initial and final relative translational energies, measured in the center-of-mass frame.[23] The quantity $E_{trans}^f$ cannot be determined from the laser-induced fluorescence spectrum. If we neglect this term, we obtain the inequality

$$D_0^0(AlO) \geq D_0^0(O_2) + E_{int}(AlO) - E_{int}(O_2) - E_{trans}^i, \quad (2)$$

which provides a lower bound to $D_0^0(AlO)$.

### A. Calculation of the initial translational energy distribution

Because the Al beam is generated at high temperatures, the spread in $E_{trans}^i$ is large, and its determination represents the major source of uncertainty in our lower bound to $D_0^0(AlO)$. Previously several ways of estimating $E_{trans}^i$ have been presented.[2,4,22] We derive here the distribution of $E_{trans}^i$ and then discuss what best value to use in Eq. (2).

In our experimental arrangement, an effusive Al beam passes through a static gas of $O_2$. Let $\mathbf{v}_1$ denote the velocity of an Al atom, and $\mathbf{v}_2$ the velocity of an $O_2$ molecule, in the laboratory frame. Then the relative velocity $\mathbf{g}$ (in the center-of-mass frame) is related to $\mathbf{v}_1$ and $\mathbf{v}_2$ by

$$g^2 = v_1^2 + v_2^2 - 2v_1v_2\cos\theta, \quad (3)$$

where $\theta$ is the angle between $\mathbf{v}_1$ and $\mathbf{v}_2$ (see Fig. 6). For the effusive Al beam, the beam density for velocities between $v_1$ and $v_1 + dv_1$ is[24]

$$f_1(v_1)dv_1 = (4v_1^2\alpha_1^{-3}\pi^{-1/2})\exp(-v_1^2/\alpha_1^2)dv_1, \quad (4)$$

where

$$\alpha_1^2 = 2kT(Al)/m(Al). \quad (5)$$

For the static $O_2$ gas, the density of $O_2$ molecules for velocities between $\mathbf{v}_2 = (v_2, \theta, \varphi)$ and $\mathbf{v}_2 + d\mathbf{v}_2$ is

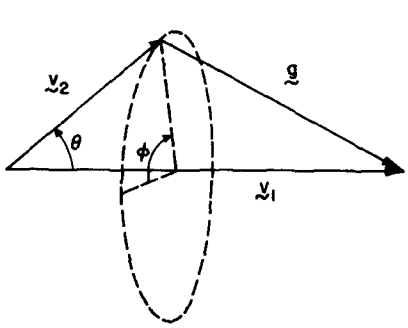


FIG. 6. Coordinates defining the velocities $v_1$ and $v_2$. Here $v_1$ is the velocity of an Al atom and is in the direction of the Al beam. The velocity $v_2$ of an $O_2$ molecule in the scattering gas is specified by $(v_2, \theta, \varphi)$. The relative velocity is $g$.

TABLE IV. Experimental determinations of the AlO $X\,^2\Sigma^+$ dissociation energy.

| Investigator | Method | $D_0^0$ (AlO) (kcal/mole) |
|---|---|---|
| Lessheim and Samuel[a] | Birge–Sponer extrapolation | 96 |
| Roy[b] | Birge–Sponer extrapolation | 93 |
| Coheur-Dehalu[c] | predissociation | 87 |
| Rosen[d] | predissociation | 21 |
| Gurvich and Viets[e] | flame photometry | 137 ± 4 |
| Drowart, DeMaria, Burns, and Inghram[f] | mass spectrometry | 115 ± 5 |
| Burns[g] | mass spectrometry | 116 ± 3 |
| Tyte[h] | long wavelength absorption limit | ≤ 104.7 ± 0.2 |
| McDonald and Innes[i] | long wavelength absorption limit | ≤ 119.9 |
| Newman and Page[j] | flame photometry | 145 ± 6 |
| Farber, Srivastava, and Uy[k] | mass spectrometry | 121 ± 4 |
| Jensen and Jones[l] | flame photometry | 142 |
| Gole and Zare[m] | chemiluminescence | ≥ 118.3 ± 1.4 |
| Hildenbrand[n] | mass spectrometry | 118.6 ± 2.5 |
| Drowart[o] | long wavelength absorption limit | ≤ 122.1 ± 0.6 |
| Frank and Krauss[p] | flame photometry | 116.8 ± 1.8 |
| Dagdigian, Cruse, and Zare[q] | laser induced fluorescence | 121.5 ± 1 |

[a] H. Lessheim and R. Samuel, Z. Phys. **84**, 637 (1933).
[b] D. Roy, Ind. J. Phys. **13**, 231 (1939).
[c] F. Coheur-Dehalu, Bull. Acad. Roy. Belg. **23**, 604 (1937).
[d] B. Rosen, Phys. Rev. **68**, 124 (1945).
[e] L. V. Gurvich and I. V. Viets, Bull. Acad. Sci., USSR, Phys. Ser. **22**, 670 (1958). See also L. V. Gurvich and I. V. Viets, Dokl. Akad. Nauk SSSR **108**, 659 (1956).
[f] J. Drowart, G. DeMaria, R. P. Burns, and M. G. Inghram, J. Chem. Phys. **32**, 1366 (1960). See also G. DeMaria, J. DeMaria, J. Drowart, and M. G. Inghram, *ibid.* **30**, 318 (1959).
[g] R. P. Burns, J. Chem. Phys. **44**, 3307 (1966).
[h] D. C. Tyte, Ref. 20.
[i] J. K. McDonald and K. K. Innes, J. Mol. Spectrosc. **32**, 501 (1969).
[j] R. N. Newman and F. M. Page, Combust. Flame **15**, 317 (1970).
[k] M. Farber, R. D. Srivastava, and O. M. Uy, Ref. 26.
[l] D. E. Jensen and G. A. Jones, J. Chem. Soc. Faraday Trans. I **68**, 259 (1972).
[m] J. L. Gole and R. N. Zare, Ref. 22.
[n] D. L. Hildenbrand, Ref. 27.
[o] J. Drowart, Ref. 21.
[p] P. Frank and L. Krauss, Z Naturforsch. **29a**, 742 (1974).
[q] This work.

$$f_2(\mathbf{v}_2)d\mathbf{v}_2 = (v_2^2\alpha_2^{-3}\pi^{-3/2})\exp(-v_2^2/\alpha_2^2)d\mathbf{v}_2, \quad (6)$$

where

$$\alpha_2^2 = 2kT(O_2)/m(O_2). \quad (7)$$

In Eqs. (5) and (7), $T$ denotes the temperature and $m$ the mass.

Since the initial relative translational energy $E_{trans}^i$ equals $\frac{1}{2}\mu g^2$, where

$$\mu = m(Al)m(O_2)/[m(Al) + m(O_2)]$$

is the reduced mass, the probability that $E^i_{trans}$ lies between $E$ and $E+dE$ is

$$p(E)dE = P(g^2)d(g^2), \tag{8}$$

where

$$P(g^2)d(g^2) = f_1(v_1)f_2(\mathbf{v}_2)dv_1 d\mathbf{v}_2. \tag{9}$$

We may obtain $P(g^2)$ for any particular value $g_0$ by substituting the velocity distributions $f_1(v_1)$ and $f_2(\mathbf{v}_2)$ into Eq. (9), multiplying both sides by $\delta(g^2 - g_0^2)$, and integrating over all velocity space. For the particular distributions appropriate to a "beam-gas" arrangement [Eqs. (4) and (6)], we find (see the Appendix)

$$P(g_0^2) = \{2g_0[\pi(\alpha_1^2+\alpha_2^2)^3]^{-1/2}\}\exp[-g_0^2/(\alpha_1^2+\alpha_2^2)], \tag{10}$$

from which the energy distribution is determined to be

$$p(E) = 2[E/\pi E_\alpha^3]^{1/2}\exp(-E/E_\alpha), \tag{11}$$

where

$$E_\alpha = \tfrac{1}{2}\mu(\alpha_1^2+\alpha_2^2). \tag{12}$$

The quantity $E_\alpha$ proves particularly useful for characterizing the relative translational energy distribution in a "beam-gas" arrangement. The average energy is given by

$$\bar{E} = \int_0^\infty Ep(E)dE = \tfrac{3}{2}E_\alpha, \tag{13}$$

while the most probable energy is given by

$$E_{mp} = \tfrac{1}{2}E_\alpha. \tag{14}$$

Moreover, the magnitude of $E_\alpha$ determines the rate of falloff of $p(E)$ at high $E$. For many reactions, $E_\alpha$ is much smaller than for $Al+O_2$; for example, $E_\alpha$ for $Ba+O_2$ is 0.9 kcal/mole,[4] while for $Al+O_2$ it is 2.0 kcal/mole. This factor of 2 change, which occurs in the exponent of $p(E)$, is caused principally by the lightness of the Al atom.

Figure 7 shows the translational energy distribution for the Al and $O_2$ collision partners under our conditions [$T(Al) = 1600\,^\circ K$, $T(O_2) = 300\,^\circ K$]. While $E_{mp}$ is only 1.0 kcal/mole, it can be seen that the distribution is very broad. For example, one collision in ten has more energy than $2\bar{E} = 6.0$ kcal/mole. This large spread becomes the main source of error in determining $D_0^0(AlO)$. Care must be taken since collisions with large $E^i_{trans}$ may be the mechanism for populating the highest AlO internal states seen.

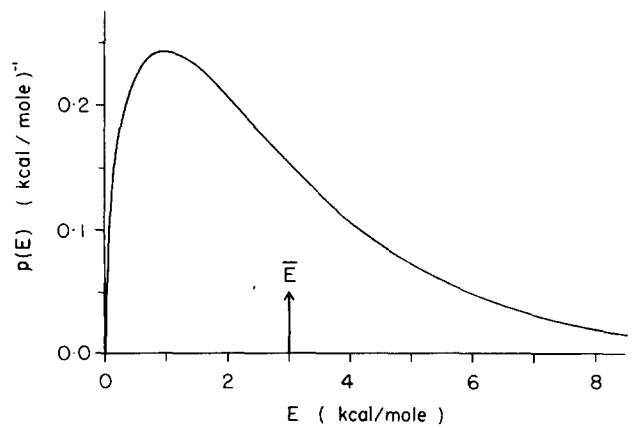


FIG. 7. Initial relative translational energy distribution for $Al+O_2$ in a "beam-gas" arrangement. The effusive Al beam has temperature $T(Al) = 1600\,^\circ K$, while the $O_2$ scattering gas is at $T(O_2) = 300\,^\circ K$. The average energy $\bar{E}$ is marked.

In a preliminary analysis[2] of this data, $E^i_{trans}$ was estimated to be 4.6 kcal/mole by assuming a head-on collision with Al and $O_2$ having their most probable velocities. This conservative estimate yields a lower bound of $D_0^0(AlO) \geq 120.6 \pm 0.9$ kcal/mole. A more satisfying estimate of $E^i_{trans}$ would seem to be to equate $E^i_{trans}$ with $\bar{E} = 3.0$ kcal/mole, since this reaction appears to have no activation energy,[1] and it is this value which is used here.

### B. Calculation of the AlO dissociation energy

In evaluating the terms in Eq. (2), we take $D_0^0(O_2)$ to be equal to $117.97 \pm 0.1$ kcal/mole,[25] and we set $E_{int}(O_2)$ equal to $RT(O_2)$, which is the average thermal energy of a diatomic rotor (vibrational excitation is negligible at room temperature). The only remaining unknown quantity in Eq. (2) is the internal energy of the AlO product, $E_{int}(AlO)$. We estimate this quantity from the AlO vibrational and rotational distributions presented in Table I and Fig. 4. The identification of $E^i_{trans}$ with $\bar{E}$ requires that we find the highest internal state populated from collisions with relative translational energies $E^i_{trans} \leq \bar{E}$, not from those collisions with $E^i_{trans} > \bar{E}$.

Examination of the vibrational distribution (Fig. 5) shows that the $v=2$ level appears to satisfy this condition, leading to the bound $D_0^0(AlO) \geq 119.9$ kcal/mole if we ignore the rotational excitation present in this vibrational level. On the other hand, the $v=4$ level does not appear to satisfy these conditions, and its use yields $D_0^0(AlO) \geq 125.2$ kcal/mole, which exceeds the upper limit placed by Drowart.[21] The intermediate choice, the $v=3$ level, provides the estimate $D_0^0(AlO) \geq 122.6$ kcal/mole, which almost coincides with Drowart's upper bound. Perhaps a superior choice can be made by taking into account the rotational excitation present in a vibrational level (Fig. 4). If we assume that the $v=1$, $N=50$ level is the highest populated, we obtain $D_0^0(AlO) \geq 121.8$ kcal/mole. Let us now revise the estimate from the $v=2$ level to include rotational excitation. The (1, 2) and (3, 2) bandheads are clearly discernible in Figs. 1 and 2, and the $N$ value at the head is about 20. Assuming that the $v=2$, $N=20$ level is the highest populated, we find $D_0^0(AlO) \geq 120.7$ kcal/mole. Considering the range of the lower bounds in which we have confidence and accepting Drowart's upper bound, we conclude that the AlO dissociation energy is

$$D_0^0(AlO) = 121.5 \pm 1 \text{ kcal/mole}. \tag{15}$$

This seems to be in excellent accord with the most recent mass spectrometric determinations by Farber, Srivastava, and Uy[26] and by Hildenbrand.[27] It will be possible in future experiments to reduce even further the uncertainty in $D_0^0(AlO)$ by velocity selecting the incident Al beam, thereby reducing the spread in the relative translational energy of the reactants.

TABLE V. Potential parameters and van der Waals constants used in phase space theory.

| | $C^{(6)}(10^{-60}$ erg cm$^6)$ | $\alpha$(Å$^3$) | $\mu$(D) |
|---|---|---|---|
| Reactants | 137 | | |
| Al | | 6[a] | |
| $O_2$ | | 1.62[b] | |
| Products | 155 | | |
| AlO | | 7.2[c] | 4.544[d] |
| O | | 0.77[b] | |

[a]Estimated from $\alpha(B)=5.1$ Å$^3$ [A. Dalgarno, Adv. Phys. **11**, 281 (1962)].
[b]R. A. Alpher and D. R. White, Phys. Fluids 2, 153 (1959).
[c]The sum of the ionic polarizabilities, $\alpha(Al^+)$ and $\alpha(O^-)$ [S. A. Adelman and A. Szabo, J. Chem. Phys. 58, 687 (1973); A. Dalgarno, footnote a].
[d]Calculated value of $\mu_0$ (Ref. 19).

## VI. AlO + $O_2$ REACTION DYNAMICS

It is of considerable interest to compare the molecular dynamics of the $Al+O_2$ reaction with other metal atom oxidation reactions. Two other $M+O_2$ systems which have been studied in detail show evidence for long-lived collision complexes. Ham and Kinsey[28] found that the angular distribution of elastically scattered K atoms from the endothermic $K+O_2$ reaction exhibits a shoulder at large laboratory scattering angles superimposed on the normal rapid falloff of elastic scattering. This shoulder is interpreted as indicative of complex formation. The well-known[29] stable $K^+O_2^-$ peroxide presumably provides a potential well in which the K and $O_2$ collision partners can be trapped.

The angular distribution of BaO formed from the exothermic $Ba+O_2$ reaction shows the forward–backward symmetry (in the center-of-mass system) expected from reactive collisions involving long-lived complexes.[30] Loesch and Herschbach[31] point out that the long lifetime of the complex can be attributed to an attractive basin in the potential surface, which may be identical to the ionic $Ba^+O_2^-$ free molecule inferred from matrix-isolation infrared studies.[32] The BaO internal state distribution from $Ba+O_2$ has also been investigated. Using laser fluorescence detection, Dagdigian, Cruse, Schultz, and Zare[4] found that the BaO rotational distribution is in remarkable agreement with that predicted by phase space theory.[33]

There are no angular distribution measurements available for the $Al+O_2$ reaction that can provide information complementary to that obtainable from laser fluorescence studies. Moreover, no potential energy surface or classical trajectory calculations have been made for this system. Accordingly, we are led to compare the AlO internal state distribution with that calculated by phase space theory for a qualitative understanding of the reaction dynamics. While phase space theory makes no assumptions about the lifetime of the collision complex, the BaO results strongly suggest that when a long-lived complex is involved, the excess energy of the M + $O_2$ reaction is partitioned "statistically."

The application of phase space theory requires little detailed knowledge about the potential energy surface. The dissociation of the collision complex is assumed to be governed solely by the conservation of angular momentum and energy. As with the previous calculations[4] on $Ba+O_2$ and $Ba+CO_2$, we take the long-range interaction energy for both reactant and product channels to be the sum of a Slater–Kirkwood dispersion term[34] and an induction term[35] of the form $V(r)=-C^{(6)}r^{-6}$, and we assume there are no activation barriers. The parameters used and the resulting $C^{(6)}$ constants are listed in Table V. The dissociation energy $D_0^0$(AlO) is taken to be 122 kcal/mole, and the reactants are assumed to be in their lowest internal states.

Because of the large spread in the initial relative translational energy $E^i_{trans}$, two different ways of estimating an average $E$ are used. The first and simplest means is to take the average value $\bar{E}=3.0$ kcal/mole calculated earlier (Sec. V A). The solid curves in Fig. 8 illustrate the rotational distributions calculated by phase space theory for AlO molecules formed in the $v=0$ (a) and $v=1$ (b) levels, for this choice. Comparison with the experimental results in Fig. 4 reveal that the experimental and calculated distributions differ significantly and that the calculation predicts too much rotational excitation. A superior way of accounting for the spread in $E$ is to calculate the internal state distribution for several values of $E^i_{trans}$ and then to average in a weighted manner. We have calculated the cross sections

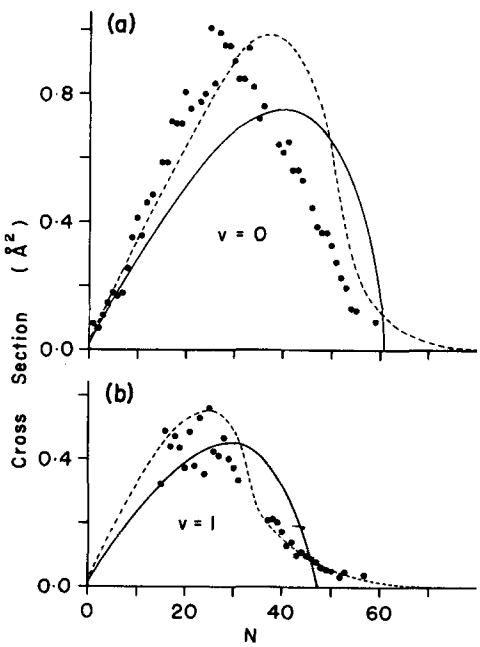


FIG. 8. Rotational populations calculated by phase space theory for AlO molecules produced in the (a) $v=0$ and (b) $v=1$ vibrational levels from the $Al+O_2$ reaction. The solid lines are calculated assuming $E^i_{trans}=3.0$ kcal/mole, the average initial relative translational energy, while the dashed lines are obtained from a thermal averaging using $p(E)$ given in Fig. 7. For comparison, the experimentally determined rotational populations are also plotted and are arbitrarily normalized so that the population of the $v=0$, $N=30$ level is the same as that calculated by phase space theory with thermal averaging.

$\sigma_{vN}$ for formation of the AlO $(v, N)$ level at $E = 1, 3, 5, 7$, and 9 kcal/mole. The dashed curves in Fig. 8 represent the weighted average

$$\langle \sigma_{vN} \rangle = \sum_i w(E_i)\sigma_{vN}(E_i), \tag{16}$$

where the weight $w(E_i)$ is the probability $p(E)$ averaged over a 2 kcal/mole wide interval centered on $E_i$:

$$w(E_i) = \int_{E_i-1}^{E_i+1} p(E)dE. \tag{17}$$

By substituting for $p(E)$ the expression given in Eq. (11), we find

$$w(E_i) = \mathrm{erf}\left[\left(\frac{E_i+1}{E_\alpha}\right)^{1/2}\right] - \mathrm{erf}\left[\left(\frac{E_i-1}{E_\alpha}\right)^{1/2}\right] - 2(\pi E_\alpha)^{-1/2} \times \left[(E_i+1)^{1/2}\exp\left(-\frac{E_i+1}{E_\alpha}\right) - (E_i-1)^{1/2}\exp\left(-\frac{E_i-1}{E_\alpha}\right)\right], \tag{18}$$

where $E_\alpha$ is defined as in Eq. (12). It can be seen that these thermally averaged calculations agree more closely with the experimental results. The $v = 1$ distributions are very similar to within the expected experimental uncertainties, while the calculations still predict significantly more rotational excitation than is observed for the $v = 0$ level.

A thermally averaged vibrational distribution has also been calculated from phase space theory. The relative vibrational populations (normalized to the $v = 0$ level) are $N_0 : N_1 : N_2 : N_3 : N_4 = (1.00) : 0.431 : 0.0412 : 0.0048 : 0.0004$. Comparison with the experimental distribution listed in Table I shows that the $N_1/N_0$ ratio is predicted rather well but that the calculated distribution falls off too rapidly with increasing $v$. The discrepancies in the $v = 0$ rotational distribution and the vibrational distribution suggest that the Al + $O_2$ reaction energy is not distributed entirely "statistically" among the various AlO degrees of freedom. At first glance, this may seem surprising in view of the fact that $AlO_2$ is a stable high-temperature species. Based on the investigations of the Ba + $O_2$ reaction,[4,30] we expect statistical behavior to be correlated with a long-lived complex. However, $AlO_2$ is expected to have a linear O–Al–O structure, in analogy to the ground state structure of $BO_2$.[26] Thus, we believe that the Al + $O_2$ reaction does not proceed through the O–Al–O intermediate because it would be very difficult for the reactants to reach this attractive well. Although the molecule Al–$O_2$ may have bound states, the nonstatistical product distribution suggests that the Al + $O_2$ reaction most probably proceeds, at least in part, by a direct mechanism. These tentative conclusions can be tested by measurement of an AlO angular distribution and by further laser fluorescence studies using a velocity-selected Al beam to narrow the spread in the initial translational energy.

## ACKNOWLEDGMENTS

We are indebted to A. Fontijn (AeroChem Research Laboratories, Inc., Princeton, New Jersey) for suggesting to us the use of boron nitride as an oven container material for aluminum, to K. K. Innes (State University of New York at Binghampton) for bringing the spectroscopic work of M. K. Sen to our attention, and to J. Drowart (Vrije Universiteit Brussel) for communicating his unpublished work on an upper bound to $D_0^0$(AlO) and for stimulating our efforts to derive the relative translational energy distribution in a "beam-gas" scattering experiment. This work has been supported, in part, by the Advanced Research Projects Agency through Grant No. DA-ARO-D-31-124-73-G82, by the Air Force Office of Scientific Research through Grant Nos. AFOSR-72-2275 and AFOSR-73-2551A, and by the Office of Naval Research through Grant No. N00014-67-A-0108-0038.

## APPENDIX: DERIVATION OF THE RELATIVE SQUARED SPEED DISTRIBUTION FOR A BEAM–GAS ARRANGEMENT

Here we outline explicitly the steps necessary to derive Eq. (10) from Eq. (9). Multiplying both sides of Eq. (9) by $\delta(g^2 - g_0^2)$ and integrating over all velocity space, we obtain

$$P(g_0^2) = \int \delta(g^2 - g_0^2)\, P(g^2)d(g^2)$$
$$= \int \delta(g^2 - g_0^2) f_1(v_1) f_2(\mathbf{v}_2) dv_1 d\mathbf{v}_2$$
$$= \int \delta(g^2 - g_0^2) f_1(v_1) f_2(v_2, \theta, \varphi) dv_1 dv_2 \sin\theta d\theta d\varphi. \tag{A1}$$

We substitute the expressions for $f_1(v_1)$ and $f_2(\mathbf{v}_2)$ from Eqs. (4) and (6), use the identity

$$\delta(g^2 - g_0^2) = \delta(v_1^2 + v_2^2 - 2v_1v_2\cos\theta - g_0^2), \tag{A2}$$

and perform the trivial integration over $\varphi$:

$$P(g_0^2) = \frac{8}{\pi\alpha_1^3\alpha_2^3}\int_0^\infty\int_0^\infty\int_0^\pi v_1^2 v_2^2 \exp\left(-\frac{v_1^2}{\alpha_1^2} - \frac{v_2^2}{\alpha_2^2}\right) \times \delta(v_1^2 + v_2^2 - 2v_1v_2\cos\theta - g_0^2) dv_1 dv_2 \sin\theta d\theta. \tag{A3}$$

Let $x = \cos\theta$. The integral over $\theta$,

$$I_\theta = \int_{-1}^{+1} \delta(v_1^2 + v_2^2 - 2v_1v_2x - g_0^2)dx, \tag{A4}$$

has the value

$$I_\theta = (2v_1v_2)^{-1} \quad \text{for } |x_0| \le 1$$
$$= 0 \quad \text{for } |x_0| > 1, \tag{A5}$$

where $x_0 = (g_0^2 - v_1^2 - v_2^2)/2v_1v_2$. This restriction on $I_\theta$ then sets limits on the integration over $v_2$:

$$P(g_0^2) = \frac{4}{\pi\alpha_1^3\alpha_2^3}\int_0^\infty\int_{|v_1-g_0|}^{v_1+g_0} v_1v_2\exp\left(-\frac{v_1^2}{\alpha_1^2} - \frac{v_2^2}{\alpha_2^2}\right)dv_1dv_2. \tag{A6}$$

The integration over $v_2$ is carried out using the identity

$$\int_0^u x\exp(-q^2x^2)dx = \frac{1 - \exp(-q^2u^2)}{2q^2}. \tag{A7}$$

We obtain, after some algebra,

$$P(g_0^2) = \frac{4}{\pi\alpha_1^3\alpha_2}\exp\left(-\frac{g_0^2}{\alpha_2^2}\right)\int_0^\infty v_1\sinh\left(\frac{2v_1g_0}{\alpha_2^2}\right) \times \exp[-v_1^2(\alpha_1^{-2} + \alpha_2^{-2})]dv_1. \tag{A8}$$

The integration over $v_1$ may then be recognized as a

tabulated integral.[36] We obtain for the final result

$$P(g_0^2) = \{2g_0[\pi(\alpha_1^2 + \alpha_2^2)^3]^{-1/2}\} \exp[-g_0^2/(\alpha_1^2 + \alpha_2^2)], \quad \text{(A9)}$$

which is Eq. (10).

*Present address: Department of Chemistry, The Johns Hopkins University, Baltimore, Md. 21218.
†Present address: Shell Research Limited, Thornton Research Centre, P. O. Box 1, Chester CHl 3SH, England.

[1]A. Fontijn, W. Felder, and J. J. Houghton, Chem. Phys. Lett. 27, 365 (1974); "Homogeneous and Heterogeneous Kinetics of the Atomic $Al/O_2$ Reaction in the 1000-1700 K Range," in Proceedings of the Fifteenth Symposium (International) on Combustion (The Combustion Institute, Pittsburgh, to be published).
[2]A preliminary report on the $Al + O_2$ reaction has appeared in R. N. Zare, Ber. Bunsenges. Physik. Chem. 78, 153 (1974).
[3]R. N. Zare and P. J. Dagdigian, Science 185, 739 (1974).
[4]P. J. Dagdigian, H. W. Cruse, A. Schultz, and R. N. Zare, J. Chem. Phys. 61, 4450 (1974).
[5]A. N. Nesmeyanov, *Vapor Pressure of the Elements*, transl. by J. I. Carrasso (Academic, New York, 1963).
[6]The source of this dye was the IBM Watson Research Center, Yorktown Heights, N. Y., and the material was made by C. S. Angadijavar and R. Srinivasan. We are grateful to R. Srinivasan for supplying us with a sample of this dye.
[7]H. W. Cruse, P. J. Dagdigian, and R. N. Zare, Faraday Disc. Chem. Soc. 55, 277 (1973).
[8]See G. Herzberg, *Spectra of Diatomic Molecules* (D. Van Nostrand, Princeton, 1950), p. 249, for a listing of the allowed branches of a $^2\Sigma^+ - ^2\Sigma^+$ band. Here K is used instead of N.
[9]RKR Franck–Condon factors $q_{v'v''}$ have been calculated for the AlO $B-X$ system by A. Sharma, J. Quant. Spectrosc. Radiat. Transfer 7, 289 (1967); H. H. Michels, J. Chem. Phys. 56, 665 (1972); and H. S. Liszt and W. H. Smith, J. Quant. Spectrosc. Radiat. Transfer 12, 947 (1972). For the bands used here, the $q_{v'v''}$ of Liszt and Smith and of Michels differ by less than 1%, while those of Sharma differ by as much as 35%. The values of Liszt and Smith are used here.
[10]Equation (1) of Ref. 4 shows the relationship between rotational populations and fluorescence intensities of individual lines.
[11]The spectroscopic data were obtained from M. K. Sen, Ind. J. Phys. 11, 251 (1937); A. Lagerqvist, N. E. L. Nilsson, and R. F. Barrow, Ark. Fys. 12, 543 (1957); and V. W. Goodlett and K. K. Innes, Nature 183, 243 (1959).
[12]While the derivation of the low $N$ behavior given in Appendix A of Ref. 4 assumed that phase space theory applies to the reaction, this behavior is in fact much more general and only requires that many $N$ levels be energetically accessible.
[13]P. J. Dagdigian, H. W. Cruse, and R. N. Zare, J. Chem. Phys. 60, 2330 (1974).
[14]M. Vanpee, W. R. Kineyko, and R. Caruso, Combust. Flame 14, 381 (1970).
[15]W. J. Hooker and R. P. Main, "AlO ($A-X$) Oscillator Strengths and Collisional Reaction Rates," Final Report, KMS Technology Center, 1971.
[16]T. Wentink, Jr., N. Pedersen, and G. Diebold, "Radiative Behavior of Metal Oxides in Laser Blowoff," DASA Report No. 2704, 1971.
[17]S. E. Johnson, G. Capelle, and H. P. Broida, J. Chem. Phys. 56, 663 (1972).
[18]H. H. Michels, J. Chem. Phys. 56, 665 (1972).
[19]M. Yoshimine, A. D. McLean, and B. Liu, J. Chem. Phys. 58, 4412 (1973).
[20]D. C. Tyte, Proc. Phys. Soc. Lond. 92, 1134 (1967).
[21]J. Drowart (Vrije Universiteit Brussel, private communication, 1973) reinterpreted the micro-densitometer tracings of Tyte (Ref. 20) and identified the absorption edges from $v = 0$ and 1 in the AlO $A\,^2\Pi_i$ state. In addition, he substantiated that the upper state potential curve is nearly horizontal so that the long-wavelength limit of absorption may be equated with the dissociation limit.
[22]J. L. Gole and R. N. Zare, J. Chem. Phys. 57, 5331 (1972).
[23]We have neglected the fine structure splittings of Al $^2P$, O $^3P$, and $O_2$ $^3\Sigma_g^-$ in this calculation since they are negligible compared to the experimental uncertainties.
[24]See, for example, N. F. Ramsey, *Molecular Beams* (Oxford University, Oxford, 1956), pp. 19–21. Our expression for $f_1(v_1)$ differs from Ramsey's [Eq. II. 26] by a power of $v$ since he is considering the beam flux and not density.
[25]B. de B. Darwent, Natl. Bur. Std. Ref. Data Ser. NSRDS-NBS 31 (1970).
[26]M. Farber, R. D. Srivastava, and O. M. Uy, J. Chem. Soc. Faraday Trans. I 68, 249 (1972); J. Chem. Phys. 55, 4142 (1971).
[27]D. L. Hildenbrand, Chem. Phys. Lett. 20, 127 (1973).
[28]D. O. Ham and J. L. Kinsey, J. Chem. Phys. 53, 285 (1970).
[29]R. R. Smardzewski and L. Andrews, J. Chem. Phys. 57, 1327 (1972); L. Andrews, *ibid.* 54, 4935 (1971).
[30]H. J. Loesch and D. R. Herschbach (to be published); F. Engelke, thesis (University of Freiburg, Germany, 1974). Earlier work includes C. B. Cosmovici and K. W. Michel, Chem. Phys. Lett. 11, 245 (1971); J. Fricke, B. Kim, and W. L. Fite, in *Proceedings of the VII ICPEAC, Abstract of Papers* (North-Holland, Amsterdam, 1971), p. 37.
[31]See D. A. Dixon, D. D. Parrish, and D. R. Herschbach, Faraday Disc. Chem. Soc. 55, 385 (1973).
[32]S. Abramowitz and N. Acquista, J. Res. Natl. Bur. Stand. (U. S.) 75A, 23 (1970).
[33]P. Pechukas, J. C. Light, and C. Rankin, J. Chem. Phys. 44, 794 (1966).
[34]J. O. Hirschfelder, C. F. Curtiss, and R. B. Bird, *Molecular Theory of Gases and Liquids* (Wiley, New York, 1954), p. 964.
[35]Reference 34, p. 987.
[36]I. S. Gradshteyn and I. M. Ryzhik, *Table of Integrals, Series, and Products* (Academic, New York, 1965), p. 365, Eq. (3.562.3).